Analytical Description of Multilevel Carrier-Based PWM of Arbitrary Bounded Input Signals

Harald Enzinger, Christian Vogel
Telecommunications Research Center Vienna (FTW), Austria
Email: enzinger@ftw.at, c.vogel@ieee.org

***Abstract*—A mathematical framework for analytical description of multilevel carrier-based pulse-width modulation (PWM) is presented. The framework does not make any assumptions on the input signal and is able to model any configuration of periodic, piecewise-linear carrier signals, specified by two line-segments. By using the framework it is shown that analytical equations can be obtained for two practically relevant multilevel PWM schemes. The derived equations simplify spectral analysis, which is exemplified by numerical simulations.**

I. Introduction

Pulse-width modulation (PWM) is a widely used form of time-encoding that maps a real-valued signal to time-varying widths of a pulse train. Many practical applications use carrier-based PWM, which can be implemented with low complexity by using a comparator and a piecewise linear carrier signal. The binary nature of PWM enables highly efficient operation of electric motor drives, switched-mode power converters [1] and switched-mode power amplifiers [2]. By combining several two-level PWM signals, multilevel PWM can be obtained, which has improved spectral characteristics.

To evaluate PWM for various applications, analytical equations for PWM are of great advantage. A classical approach [3] uses two-dimensional Fourier series analysis to describe two-level PWM for sinusoidal inputs. This approach is widely used in power electronics and can be extended to multilevel PWM [4], [5]. For the fields of audio and communications engineering a description for arbitrary input signals is required. In [6], analytical equations for two-level PWM have been derived without restriction of the input signal. However, the derivations in [6] are complicated and not well suited for an extension to multilevel PWM. In [7], a partial Fourier series analysis was used to describe two-level PWM for arbitrary input signals and in [8] it was shown that this approach can also be applied to a specific multilevel PWM scheme.

This work extents the approach from [7] to a general framework for the analysis of multilevel carrier-based PWM. By using the framework it is shown that analytical equations can be derived for two practically relevant multilevel PWM schemes and that both can produce the same multilevel output.

The research leading to these results has received funding from the FFG Competence Headquarter program under the project number 835187. The Austrian Competence Center FTW Forschungszentrum Telekommunikation Wien GmbH is funded within the program COMET - Competence Centers for Excellent Technologies by BMVIT, BMWFJ, and the City of Vienna. The COMET program is managed by the FFG.

II. System Model

The following analysis describes carrier-based PWM as a mapping from a continuous-time, continuous-amplitude input signal $a(t)$ to a continuous-time, discrete-amplitude output signal $p(t)$ by using the system model in Fig. 1.

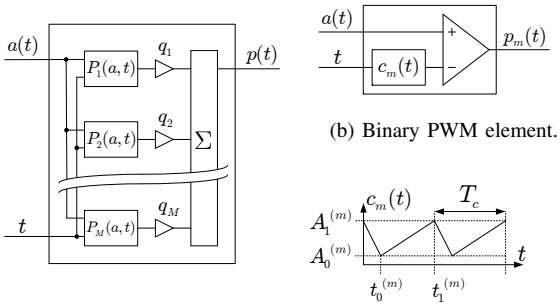

(a) Multilevel PWM system. (b) Binary PWM element. (c) Piecewise-linear carrier.

Fig. 1. System model for multilevel carrier-based PWM.

The mapping of the multilevel PWM system in Fig. 1a is described by a two-dimensional function $P(a,t)$ such that

$$p(t) = P(a(t), t) \tag{1}$$

The function $P(a,t)$ is formed by a linear combination of M binary PWM functions $P_m(a,t)$ given by

$$P(a,t) = \sum_{m=1}^{M} q_m P_m(a,t) \tag{2}$$

with q_m being weighting factors and $P_m(a,t)$ being implemented according to Fig. 1b expressed by

$$P_m(a,t) = \begin{cases} 1 & a \geq c_m(t) \\ 0 & a < c_m(t) \end{cases} \tag{3}$$

The carrier signals $c_m(t)$ are defined according to Fig. 1c as periodic, piecewise-linear functions, connecting the points $c_m(t_0^{(m)}) = A_0^{(m)}$, $c_m(t_1^{(m)}) = A_1^{(m)}$ and $c_m(t_0^{(m)} + T_\mathrm{c}) = A_0^{(m)}$ with T_c being the carrier period such that

$$c_m(t) = c_m(t + nT_\mathrm{c}) \quad \forall n \in \mathbb{Z} \tag{4}$$

By inserting (4) into (3) it can be shown that also the two dimensional function $P_m(a,t)$ is periodic in the time-dimension expressed by

$$P_m(a,t) = P_m(a, t + nT_\mathrm{c}) \quad \forall n \in \mathbb{Z} \tag{5}$$

III. Partial Fourier Series Analysis

Because of the periodicity stated in (5), the function $P_m(a,t)$ can be partially expanded into a Fourier series by

$$P_m(a,t) = \sum_{k=-\infty}^{+\infty} c_k^{(m)}(a) e^{j\frac{2\pi}{T_c}kt} \tag{6}$$

with the complex Fourier coefficients

$$c_k^{(m)}(a) = \frac{1}{T_c}\int_{t_0-\frac{T_c}{2}}^{t_0+\frac{T_c}{2}} P_m(a,t) e^{-j\frac{2\pi}{T_c}kt} dt \tag{7}$$

The integration in (7) is performed over one carrier-period of the time-dimension with an arbitrary center t_0. With the piecewise-linear carrier of Fig. 1c, there is exactly one pulse per carrier-period for a specific input a. Therefore the integral can be evaluated by setting t_0 to the pulse center $\tau_m(a)$ and symmetrically integrating over the time-duration for which $P_m(a,t)$ is equal to 1, which is given by the duty cycle $d_m(a)$. With these substitutions (7) can be written as

$$c_k^{(m)}(a) = \frac{1}{T_c}\int_{\tau_m(a)-d_m(a)\frac{T_c}{2}}^{\tau_m(a)+d_m(a)\frac{T_c}{2}} e^{-j\frac{2\pi}{T_c}kt} dt \tag{8}$$

with the pulse center

$$\tau_m(a) = t_0^{(m)} + \left(t_1^{(m)} - t_0^{(m)} - \frac{T_c}{2}\right) d_m(a) \tag{9}$$

and the duty cycle

$$d_m(a) = \begin{cases} 0 & a < A_0^{(m)} \\ \frac{a-A_0^{(m)}}{A_1^{(m)}-A_0^{(m)}} & A_0^{(m)} \le a \le A_1^{(m)} \\ 1 & a > A_1^{(m)} \end{cases} \tag{10}$$

An evaluation of (8) for $k = 0$ results in

$$c_0^{(m)}(a) = d_m(a) \tag{11}$$

and an evaluation of (8) for $k > 0$ results in

$$c_k^{(m)}(a) = \frac{1}{\pi k}\sin\left(\pi k d_m(a)\right) e^{-j\frac{2\pi}{T_c}k\tau_m(a)} \tag{12}$$

Since the multilevel PWM output is formed by a linear combination of binary PWM outputs, also the multilevel PWM model can be described by a Fourier series given by

$$P(a,t) = \sum_{k=-\infty}^{+\infty} c_k(a) e^{j\frac{2\pi}{T_c}kt} \tag{13}$$

with the coefficients for $k = 0$

$$c_0(a) = \sum_{m=1}^{M} q_m d_m(a) \tag{14}$$

and the coefficients for $k > 0$

$$c_k(a) = \sum_{m=1}^{M} q_m \frac{1}{\pi k}\sin\left(\pi k d_m(a)\right) e^{-j\frac{2\pi}{T_c}k\tau_m(a)} \tag{15}$$

As the output of the multilevel PWM model is real-valued, the complex Fourier coefficients are symmetric such that c_k is equal to c_{-k}^*. Accordingly, the terms for positive and negative k in (13) can be combined leading to

$$P(a,t) = c_0(a) + \sum_{k=1}^{+\infty} 2\Re\left\{c_k(a) e^{j\frac{2\pi}{T_c}kt}\right\} \tag{16}$$

By further evaluation, (16) can be either transformed to a polar representation given by

$$P(a,t) = c_0(a) + \sum_{k=1}^{+\infty} 2|c_k(a)|\cos\left(\frac{2\pi}{T_c}kt + \angle c_k(a)\right) \tag{17}$$

or a Cartesian representation given by

$$\begin{aligned} P(a,t) = c_0(a) &+ \sum_{k=1}^{+\infty} 2\Re\left\{c_k(a)\right\}\cos\left(\frac{2\pi}{T_c}kt\right) \\ &- 2\Im\left\{c_k(a)\right\}\sin\left(\frac{2\pi}{T_c}kt\right) \end{aligned} \tag{18}$$

From (17) and (18) it can be seen that the multilevel PWM signal consists of a low-pass component $c_0(a)$ and carrier harmonics at integer multiples of the carrier frequency $f_c = 1/T_c$, which are complex modulated according to $c_k(a)$. In (17) the complex modulation is expressed by an amplitude modulation given by $2|c_k(a)|$ and a phase modulation given by $\angle c_k(a)$. In (18) the complex modulation is expressed by two amplitude modulations given by $2\Re\{c_k(a)\}$ and $2\Im\{c_k(a)\}$.

IV. Multilevel PWM Schemes

Based on the choice of parameters $A_0^{(m)}$, $A_1^{(m)}$, $t_0^{(m)}$, $t_1^{(m)}$ and q_m for $m = 1 \ldots M$ many different multilevel PWM schemes are possible. In the following two special cases are investigated and it is shown that the multilevel output signal of both schemes can be described by the same analytical equation. In both cases triangular shaped carrier signals are assumed which is known as double-edge modulation [6] and results from setting $t_1^{(m)} = t_0^{(m)} + \frac{T_c}{2}$. Additionally it is assumed that the input/output range is $[0,1]$ and that the input signal $a(t)$ is limited within this range. The weighting factors q_m are set to $1/M$ for both schemes.

The first scheme will be called amplitude-slicing and results from dividing the amplitude range into M uniform and contiguous slices [4]. Each of the M carriers sweeps within one of the slices and the phases of neighboring carriers are set to opposite values. An example is depicted in Fig. 2a and the parameters are given in Table I.

The second scheme will be called phase-interleaving and results from uniformly distributing the carrier-phases between 0 and 2π [9]. Unlike to amplitude-slicing, each carrier sweeps over the full amplitude range and the carrier frequency is set M times lower than the desired pulse frequency. An example is depicted in Fig. 2b and the parameters are given in Table I.

For both schemes, analytical equations are obtained by evaluating the multilevel Fourier coefficients given in (14) and (15) and inserting the results into (18). For this purpose, the pulse center in (9) and the duty cycle in (10) are evaluated with the respective parameters from Table I.

TABLE I
PARAMETERS FOR MULTILEVEL PWM SCHEMES.

	$A_0^{(m)}$	$A_1^{(m)}$	$t_0^{(m)}$	$t_1^{(m)}$
Amplitude-Slicing	$\frac{m-1}{M}$	$\frac{m}{M}$	$(m-1)\frac{T_\mathrm{c}}{2}$	$t_0^{(m)} + \frac{T_\mathrm{c}}{2}$
Phase-Interleaving	0	1	$\frac{m-1}{M}T_\mathrm{c}$	$t_0^{(m)} + \frac{T_\mathrm{c}}{2}$

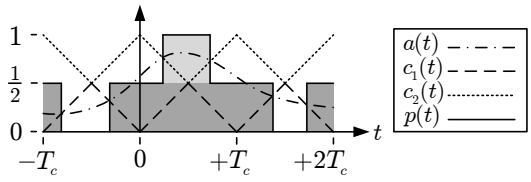

(a) Amplitude-slicing PWM for $M = 2$.

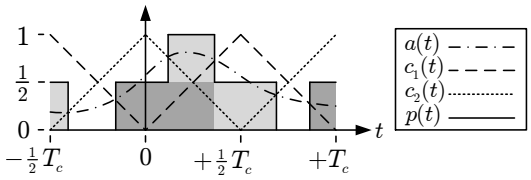

(b) Phase-interleaving PWM for $M = 2$.

Fig. 2. Multilevel PWM schemes.

A. Amplitude-Slicing

With the amplitude-slicing parameters from Table I, it can be shown that (14) reduces to $c_0(a) = a$ for $a \in [0, 1]$. By inserting the parameters into (15) it leads to

$$c_k(a) = \sum_{m=1}^{M} \frac{1}{\pi}\frac{1}{kM} \sin\left(\pi k d_m(a)\right) e^{-j\pi k(m-1)} \tag{19}$$

Since with amplitude slicing the duty cycle $d_m(a)$ has a constant value of 0 or 1 outside of the respective amplitude slice, (19) can be evaluated for each amplitude slice individually. By noting that the exponential term in (19) cancels the phase jumps between amplitude slices, (19) can be reduced to

$$c_k(a) = \frac{1}{\pi}\frac{1}{kM} \sin\left(\pi k M a\right) \tag{20}$$

The multilevel PWM model for amplitude-slicing is therefore described by

$$P(a,t) = a + \sum_{k=1}^{+\infty} \frac{2}{\pi}\frac{1}{kM} \sin\left(\pi k M a\right) \cos\left(\frac{2\pi}{T_\mathrm{c}} k t\right) \tag{21}$$

B. Phase-Interleaving

With the phase-interleaving parameters from Table I, it can be shown that (14) again reduces to $c_0(a) = a$ for $a \in [0, 1]$. By inserting the parameters into (15) it leads to

$$c_k(a) = \sum_{m=1}^{M} \frac{1}{\pi}\frac{1}{kM} \sin\left(\pi k d_m(a)\right) e^{-j2\pi k \frac{m-1}{M}} \tag{22}$$

Since the duty cycle mapping is the same for all binary PWM elements, (22) can be simplified to

$$c_k(a) = \frac{1}{\pi}\frac{1}{kM} \sin\left(\pi k a\right) \sum_{m=1}^{M} \left[e^{-j2\pi \frac{k}{M}}\right]^{m-1} \tag{23}$$

By evaluating the finite geometric series in (23), it can be shown that only coefficients with k being an integer multiple of M remain such that

$$c_k(a) = \begin{cases} \frac{1}{\pi}\frac{1}{k} \sin\left(\pi k a\right) & \mathrm{mod}(k, M) = 0 \\ 0 & \text{otherwise} \end{cases} \tag{24}$$

The multilevel PWM model for phase-interleaving is therefore described by

$$P(a,t) = a + \sum_{\substack{k=nM \\ n\in\mathbb{N}}}^{+\infty} \frac{2}{\pi}\frac{1}{k} \sin\left(\pi k a\right) \cos\left(\frac{2\pi}{T_\mathrm{c}} k t\right) \tag{25}$$

By changing the summation variable in (25) it follows that

$$P(a,t) = a + \sum_{k=1}^{+\infty} \frac{2}{\pi}\frac{1}{kM} \sin\left(\pi k M a\right) \cos\left(\frac{2\pi}{T_\mathrm{c}} k M t\right) \tag{26}$$

which is the same result as (21), except for the factor M within the cosine term. This shows that phase-interleaving generates the same multilevel PWM output signal as amplitude-slicing with an M times lower carrier frequency, which is also indicated by the examples in Fig. 2.

C. Unified Description

The equivalence of the multilevel output signal for amplitude-slicing and phase-interleaving allows a unified description of both schemes given by

$$P(a,t) = a + \sum_{k=1}^{+\infty} A_{\{k\cdot M\}}(a) \cos\left(\frac{2\pi}{T_\mathrm{p}} k t\right) \tag{27}$$

with the amplitude modulation function $A_k(a)$ given by

$$A_k(a) = \frac{2}{\pi}\frac{1}{k} \sin\left(\pi k a\right) \tag{28}$$

and the multilevel pulse period T_p equal to T_c for amplitude-slicing and T_c/M for phase-interleaving.

A bipolar input/output range can easily be obtained by applying affine transformations on the input/output signals before and after the PWM. This does not change the spectral characteristics of the harmonics but leads to a different representation of the amplitude modulation function $A_k(a)$. In the case of a bipolar input/output range of $[-1, +1]$, it changes to

$$A_k(a) = \frac{4}{\pi}\frac{1}{k} \sin\left(\pi k \frac{a+1}{2}\right) \tag{29}$$

which can be transformed to

$$A_k(a) = \begin{cases} \frac{4}{\pi}\frac{1}{k} \cos\left(\frac{\pi}{2} k a\right) (-1)^{\frac{k-1}{2}} & \text{k is odd} \\ \frac{4}{\pi}\frac{1}{k} \sin\left(\frac{\pi}{2} k a\right) (-1)^{\frac{k}{2}} & \text{k is even} \end{cases} \tag{30}$$

D. Discussion

Although amplitude-slicing and phase-interleaving result in the same multilevel output signal, the individual binary switching signals are different. This can be seen from Fig. 2, were output-contributions from $p_1(t)$ are marked by dark areas and output-contributions from $p_2(t)$ are marked by light areas. In the case of amplitude-slicing, a binary PWM element only switches if the input signal is within its amplitude range. In the case of phase-interleaving, all binary PWM elements switch with the same rate. This results in a better load-distribution in the case of phase-interleaving.

V. Evaluation of Spectra

To verify the derived equations, numerical simulations have been made. A bipolar multitone test signal with uniform amplitudes and random phases was used. The PWM pulse frequency $f_p = 1/T_\mathrm{p}$ was set to 10 times the highest frequency in the multitone signal. The sampling frequency of the numerical simulation was set to 100 times the PWM pulse frequency. The spectra were obtained by averaging over 100 input signal realizations. In the numerical simulation, the PWM system was implemented exactly how it was described in Section II. In the analytical simulation, the Fourier series equations were evaluated for each harmonic separately. The resulting spectra for two-, three-, and four-level PWM are depicted in Fig. 3.

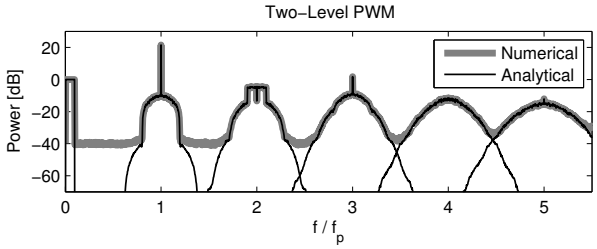

(a) Two-Level PWM.

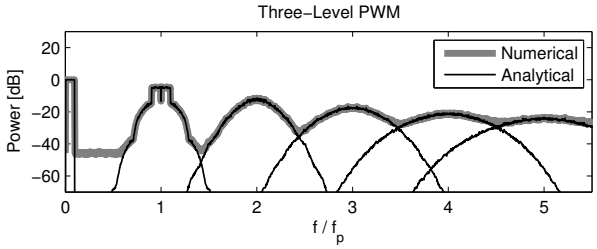

(b) Three-Level PWM.

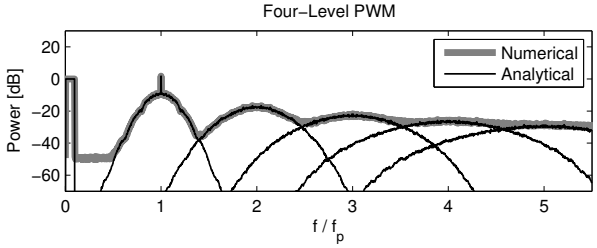

(c) Four-Level PWM.

Fig. 3. Spectra of PWM.

In Fig. 3a, the power spectrum of two-level PWM is shown. In the low-pass part of the spectrum, the input signal is present. At each multiple of the pulse frequency f_p, a distorted version of the input signal is present. The spectral regrowth at the harmonics can be modeled accurately by (30). In Fig. 3b and Fig. 3c, the spectra for three-, and four-level PWM are shown. It can be seen that the spectral regrowth at harmonic k is the same as in the case of two-level PWM at harmonic kM. This shows that by increasing the number of PWM levels, the harmonic distortion decreases in magnitude, but spreads out over wider frequency ranges. Finally it can be seen from Fig. 3, that in the numerical simulations, the dynamic range of the low-pass component is limited to 40 to 50 dB. In [7] it was shown that this results from aliasing distortion which inevitably occurs, if the not band-limited operation of PWM is implemented in a digital system. By evaluation of the analytical formulas for a limited number of harmonics, aliasing can be avoided and the spectrum of the ideal PWM signal can be obtained without the need for high oversampling.

VI. Conclusion

A mathematical framework for the spectral analysis of multilevel carrier-based PWM has been presented. The framework is based on partial Fourier series expansion which does not restrict the class of input signals. It has been shown that analytical equations can be derived for two multilevel PWM schemes, which lead to the conclusion that both can generate the same multilevel output signal. As a consequence, the discussed schemes can be interpreted as two alternative implementations of one unified multilevel PWM scheme. Additionally to the derivation of analytical equations for specific PWM schemes, the mathematical framework can be used to simulate multilevel PWM for arbitrary carrier configurations. By separate evaluation for each carrier harmonic, this gives insight into the cause of nonlinear distortion and can be used to evaluate and optimize PWM for specific applications.

References

[1] J. Holtz, "Pulsewidth modulation - a survey," *IEEE Trans. Ind. Electron.*, vol. 39, no. 5, pp. 410–420, 1992.

[2] J. Walling and D. Allstot, "Pulse-width modulated CMOS power amplifiers," *Microwave Magazine, IEEE*, vol. 12, no. 1, pp. 52–60, 2011.

[3] H. Black, *Modulation Theory*. Van Nostrand, 1953.

[4] G. Carrara, S. Gardella, M. Marchesoni, R. Salutari, and G. Sciutto, "A new multilevel PWM method: A theoretical analysis," *IEEE Trans. Power Electron.*, vol. 7, no. 3, pp. 497–505, 1992.

[5] W. Lau, B. Zhou, and H.-H. Chung, "Compact analytical solutions for determining the spectral characteristics of multicarrier-based multilevel PWM," *IEEE Trans. Circuits Syst. I*, vol. 51, no. 8, pp. 1577–1585, 2004.

[6] Z. Song and D. Sarwate, "The frequency spectrum of pulse width modulated signals," *Signal Processing*, vol. 83, no. 10, pp. 2227 – 2258, 2003.

[7] K. Hausmair, S. Chi, P. Singerl, and C. Vogel, "Aliasing-free digital pulse-width modulation for burst-mode RF transmitters," *IEEE Trans. Circuits Syst. I*, vol. 60, no. 2, pp. 415–427, 2013.

[8] K. Hausmair, S. Chi, and C. Vogel, "How to reach 100% coding efficiency in multilevel burst-mode RF transmitters," in *IEEE Int. Symp. Circuits Syst.*, 2013, pp. 2255–2258.

[9] J.-H. Chen, H.-S. Yang, H.-C. Lin, and Y.-J. Chen, "A polar-transmitter architecture using multiphase pulsewidth modulation," *IEEE Trans. Circuits Syst. I*, vol. 58, no. 2, pp. 244–252, 2011.